Modified stiffened panel analysis methods for laser beam and friction stir welded aircraft panels

Murphy, A., Lynch, F., Price, M., & Gibson, A. (2006). Modified stiffened panel analysis methods for laser beam and friction stir welded aircraft panels. Proceedings of the Institution of Mechanical Engineers, Part G: Journal of Aerospace Engineering, 220(4), 267-278. DOI: 10.1243/09544100JAERO51

Published in:
Proceedings of the Institution of Mechanical Engineers, Part G: Journal of Aerospace Engineering

Document Version:
Peer reviewed version

MODIFIED STIFFENED PANEL ANALYSIS METHODS FOR LASER BEAM AND FRICTION STIR WELDED AIRCRAFT PANELS.

A. Murphy [a, +], F. Lynch [b], M. Price [a], A. Gibson [c]

[a] School of Mechanical and Aerospace Engineering, Queen's University Belfast, Belfast, UK.

[b] Smiths Aerospace, Wobaston Road, Wolverhampton, UK.

[c] School of Aviation, Massey University, NZ.

[+] Corresponding author: *Email:* a.murphy@qub.ac.uk *Fax:* +44 (028) 9097 5576

Abstract

The introduction of advanced welding methods as an alternative joining process to riveting in the manufacture of primary aircraft structure has the potential to realise reductions in both manufacturing costs and structural weight. Current design and analysis methods for aircraft panels have been developed and validated for riveted fabrication. For welded panels, considering the buckling collapse design philosophy of aircraft stiffened panels, strength prediction methods considering welding process effects for both local buckling and post buckling behaviour must be developed and validated. This paper reports on the work undertaken to develop analysis methods for the crippling failure of stiffened panels fabricated using laser beam and friction stir welding. The work assesses modifications to conventional analysis methods and Finite Element analysis methods for strength prediction. The analysis work is validated experimentally with welded single stiffener crippling specimens. The experimental programme has demonstrated the potential static strength of laser beam and friction stir welded sheet-stiffener joints for post buckling panel applications. The work undertaken has demonstrated that the crippling behaviour of welded stiffened panels may be analysed considering standard buckling behaviour. However, stiffened panel buckling analysis procedures must be altered to account for the weld joint geometry and process altered material properties.

Keywords: Laser beam welding, friction stir welding, stiffened panels, panel crippling analysis.

1. Introduction

1.1. Background

Stiffened shell panels dominate the design of aircraft primary wing, fuselage and empennage structure. Typical panels consist of an external sheet, stiffened by both longitudinal and lateral stiffeners. As a well-matured process, riveting has dominated the assembly of aircraft panels for decades. Current numerically controlled auto-riveting machines make the process less labour intensive and operator insensitive than hand riveting. However, it is generally accepted that further development of riveted design and assembly are limited to improvements in materials. To reduce production costs, and improve productivity, airframe manufacturers are therefore considering new processing technologies such as welding **[1]**.

Although the potential of welding is recognised there are still issues to be addressed, in particular, weld induced residual stresses, distortion, and corrosion protection. Significantly both generic static strength design and analysis methods and fatigue and damage tolerance design and analysis methods are required.

This article presents development work on potential analysis methods for the prediction of static strength of laser beam and friction stir welded stiffened panel structure. The work assesses modifications to conventional analysis methods and Finite Element (FE) analysis methods for the ultimate crippling strength analysis of welded sheet-stiffener joints, accounting for the local loss of material strength due to the welding process. The analysis work is validated experimentally using single stiffener crippling specimens with geometry and materials representative of fuselage panel design for a mid-sized civil transport aircraft.

The following sub-sections briefly introduce the laser beam and friction stir welding processes, as well as associated welding process effects, which influence structural performance. The succeeding section then outlines the modified conventional analysis methods for crippling. This is followed by details of the computational analysis method. The validation experimental set-up is then introduced

before the analytical, numerical and experimental results are presented and compared. Finally, the paper concludes by assessing the accuracy of the proposed analysis methods and potential analysis enhancements.

1.2. Laser beam welding

Laser beam welding is a fusion welding process which uses a high-energy laser beam as a non-arc heat source. The principle behind the process is that the laser beam is used as an intense and focused heat source that causes the metal at the joint interface to melt and intermix, upon cooling solidification occurs and a metallurgical bond results. Initially the laser beam is focused onto the surface of the workpiece and above a certain intensity the material starts to evaporate and a keyhole is formed, Figure 1. The formation of the keyhole greatly increases the laser beam absorption and the vapour pressure inside the keyhole prevents the collapse of the molten walls. As the beam and keyhole transverses forward the molten walls at the trailing edge come together and solidify.

Laser welding technology has been around for many years but the major limitation for aircraft structures has been the ability to weld relatively thin sheets without introducing excessive distortion. With current laser welding technology a high-speed, high heat intensity beam produces a small focused heat source, resulting in reduced levels of distortion compared with other forms of welding **[2]**.

Laser beam welding requires meticulous surface cleaning to remove surface oxide films. Additionally, close fit sub-component setup clamping is required to eliminate the possibility of the small diameter laser beam passing through joint setup gaps. Equipment is not portable requiring a stable base to maintain optical alignment and electrical power and water cooling facilities. Ultimately, both operating and tooling costs are high, and the equipment requires high utilisation to be truly cost effective.

It is reported that laser beam welding can proceed at rates of up to 10000 mm per minute compared to 100 mm per minute for conventional auto riveting **[3]**. The manufacturing costs are consequently estimated to be in the region of 25% lower **[4]**. Laser beam welding however, currently requires advanced 6XXX series materials and the potential manufacturing cost saving in terms of time may be reduced by increased material costs. An alternative joining process that removes the need for expensive non-standard material types is friction stir welding **[5]**. However, reported maximum process rates for friction stir welding are 1000 mm per minute.

1.3. Friction Stir welding

The friction stir welding process is a solid state joining technique. The process utilizes local friction heating to produce continuous solid-state seams. The process joins material by plasticising and then consolidating the material around the joint line. A cylindrical, shouldered tool with a profiled probe or pin is rotated and slowly plunged into the workpiece at the start of the joint line. The probe continues rotating and traverses forward in the direction of welding. Frictional heat is generated between the wear resistant tool and the material of the workpiece. As the probe proceeds, the friction heats the surrounding material and rapidly produces a plasticised zone around the probe. This heat causes the workpiece to soften at a temperature below that of the alloy's melting temperature and typically within the material's forging temperature range. This softening allows the traversing of the probe, metal flows to the back of the probe where it is extruded/forged behind the tool. It then consolidates and cools to form the bond. To produce a full-penetration groove weld in a butt joint, the bottom of the tool must be close to the bottom of the workpiece. In order to make a lap joint, the bottom of the tool must only extend through the bottom of the top sheet and into the bottom sheet, creating a metallic bond between the two sheets. A schematic of the lap joint welding process is shown in Figure 1. The weld is left in a fine-grained, hot-worked condition with no entrapped oxides or gas porosity. A benefit of this welding process is that it allows welds to be made on standard aircraft production aluminium alloys (2XXX and 7XXX series), which cannot be readily laser beam welded. In addition, friction stir welding is a robust process tolerant technique, it has the advantage that many of the welding parameters, e.g. tool design, rotation speed and

translation speed, can be controlled in a precise manner, thus controlling the energy input into the system **[6]**. The process also requires less stringent weld preparation than required for laser beam welding.

1.4. Welding effects

In order to predict the strength of a welded assembly it is necessary to consider how the welding process affects the structural properties. First considering laser beam welding, the process results in a number of zones exhibiting varying microstructure, Figure 2. The weld metal or weld bead consists of a mixture of the melted parent material and filler material. The fusion zone is at the weld metal grain boundaries, where the parent material has been partially melted. In the solid solution zone, heating is high enough to dissolve soluble constituents, which are partially retained in the solid solution if cooling is sufficiently rapid. In the partially annealed or over-aged zone heating from welding causes precipitation and/or coalescence of soluble constituents. Finally, in the unaffected zone, heating is low and does not affect parent material properties. The transitions between zones are gradual and not distinguished by any abrupt change in microstructure.

Friction stir welds include a thermo-mechanically affected zone and a heat affected zone, Figure 2. A nugget region within the thermo-mechanically affected zone and a region at the top of the weld (the crown) consist of very fine, recrystallised grains. These regions have experienced high temperatures and extensive plastic deformation and contain much smaller grains than the parent material. Within the remaining thermo-mechanically affected zone the parent material grains will have undergone some deformation; however, due to the lesser degree of deformation and lower temperatures experienced, recrystallisation will not have taken place. Adjacent to the thermo-mechanically affected zone is a heat affected zone, similar to that in laser beam welding. As with laser beam welding the heating in the unaffected zone does not affect the parent material properties, again transitions between the zones are gradual.

For static strength analysis of welded structures (both laser beam and friction stir) it is useful to simplify these various thermally and mechanically affected zones into one, commonly termed the Heat Affected Zone (HAZ) **[7, 8]**. Generally with most metals used in fabrication, with the exception of steel, the HAZ material has lower strength than the parent material **[9]**.

1.5. Current aerospace state-of-the-art

EADS (European Aeronautic Defence and Space Company) formerly Daimler-Chrysler Aerospace, has been developing laser welding for aerospace applications since 1995. This technology is currently being demonstrated on the Airbus A318, with a fuselage panel consisting of 14 longitudinal stiffeners **[10]**. Airbus has conducted an extensive series of tests and has progressed from small 1000 mm x 1000 mm panels to full-scale barrel tests. However, little information on static strength design and analysis methods are available within the public domain. In addition, generic data and design rules for welded panels are required for process trade studies (laser beam vs. friction stir welding vs. riveting).

Current examples of friction stir welding in aerospace includes the Space Shuttle external tanks and rocket boosters and the Eclipse 500 business jet which utilizes friction stir welding in both wing and fuselage sheet-stiffener panel fabrication. To date, the majority of research on friction stir welding has concentrated on developing the welding tools and procedures for making reliable welds. Notably Lockheed-Martin Space Systems along with NASA's Langley Research Centre have investigated the static strength analysis of sheet-stiffener panels. Work documented and in the public domain includes transversely loaded lap joint specimens **[11]**, single-stiffener crippling specimens **[11]**, and multiple-stiffener compression specimens **[12]**.

The NASA crippling analysis considered identical 2090-T83 aluminium lithium specimens with single-stiffener panels fabricated using conventional riveting and lap welding. Results indicated that the welded design exhibited a higher initial buckling load, but a lower crippling failure load than the riveted design. No special analysis techniques, or material properties, were used in the

welded specimen analysis to account for welding effects. The methods developed herein aim to address this limitation by considering modified material properties in the strength analysis. For the final stage of the NASA research programme, both welded and riveted large-scale multiple-stiffener panel specimens were designed, manufactured and experimentally tested **[12]**. Both the riveted and welded specimens exhibited large initial geometric imperfections and initial sheet buckling well below the predicted values. Pre-buckling global stiffness of both panels was approximately equal, however the welded panel exhibited a lower post-buckling stiffness and a 20% lower failure load than the riveted panel. The aim of the work herein, in developing methods to account for the welding effects such as reduced material properties and induced distortions will help understand and reduce the potential performance gap between riveted and welded designs.

2. Conventional analysis methods

The design philosophy of welded panels will be the same as for riveted panels, that is to say, sheet local buckling occurring at a percentage of the ultimate load, with subsequent post-buckling failure due to buckling of the stiffeners. Within the post-buckling range, as with riveted designs, the stiffener plus an effective width of sheet **[13]** will be assumed to act as a column, independent of the buckled section of sheet. Therefore, no weld joint failure should occur before the ultimate collapse load. This is similar in philosophy to removing the potential for inter rivet buckling in a riveted panel design.

2.1. Crippling

Stiffened panels are thin-walled structures, which exhibit instabilities when loaded in shear or compression, and such structures may fail at load levels significantly lower than their material limits. Both column and column sub-element buckling are possible. Column instability involves the complete member, with there being no change in member cross-section and a buckle wavelength of the same order as the length of the column. Local column sub-element instability involves

deformation of the member cross-section, with a wavelength of the order of the cross-sectional dimensions.

Stiffener crippling is characterised by a local buckling of the cross-sectional shape of the stiffener. The start of the buckling will occur at a load below the failure load of the section, the more stable sections of the cross-section (section hard points) continue to take additional load while supporting the already buckled sections. When the hard points are restrained against any lateral movement they can continue to be loaded until the stress reaches the material yield stress; the stiffener then looses its ability to support any additional load and fails. Columns with low slenderness ratio are susceptible to crippling. Typical external panels within a civil aircraft wing or fuselage will have intermediate slenderness ratios and failure modes are characterised by combined interaction between column and column sub-element buckling modes, for example combined stiffener flexing and local flange buckling.

The structural analysis herein focuses on crippling failure as it occurs at higher stress levels than combined column and column sub-element failure. This enables analysis and testing of sheet-stiffener weld joints to stress levels approaching material yield stresses. To allow the study of crippling behaviour, specimens have been design with low slenderness ratios (approximately 10) to induce crippling failure.

2.2. Conventional crippling analysis

The analysis methods modified for the welded panels are based on conventional aerospace panel analysis procedures. The local sheet buckling and panel crippling analysis techniques are based on the methods presented in Bruhn **[14]**, NASA Astronautics Structures Manual **[15]** and the ESDU Structures Sub-series **[16]**. The analysis is based on empirical data and incorporates several simplifying assumptions. The stiffener section crippling stress is determined from individual flange and web element crippling stresses which are derived from element local buckling stresses. The

collapse load is the load required on the column (stiffener plus the effective width of sheet) to induce an average stress on the total column area equal to the calculated section crippling stress.

First the stiffener cross-section is sub-divided into flange and web plate elements. The stiffener manufacturing method (formed or extruded) is used to define plate element widths **[14]**. The sub-divided elements are assumed to be long and either have simply supported or free edge conditions. The local buckling stress of the web and flange elements is then given by:

$$f_{ELB} = \frac{k \cdot \pi^2 \cdot E_T}{12 \cdot (1 - \nu^2)} \cdot \left(\frac{t}{b}\right)^2 \quad (1)$$

where t is the thickness and b the width of the buckling element. k, the buckling coefficient, is dependant on the edge support conditions of the element and E_T is the tangent modulus of the sheet material at f_{ELB} (which is used to account for plasticity). Using a Ramberg-Osgood fit the tangent modulus at a stress f is given by:

$$E_T = E\left[1 + \left(\frac{f}{f_n}\right)^{m-1}\right]^{-1} \quad (2)$$

where E, m and f_n are determined material properties **[17]**. Equation (1) and (2) are required to be solved iteratively. The crippling stress of an element may then be calculated using its local buckling stress, the material compressive yield stress, f_{CY}, and Equation 3:

$$f_{ECR} = \sqrt{f_{ELB} \cdot f_{CY}} \quad (3)$$

Finally, the crippling stresses of the stiffener section may be determined using a weighted average calculation based on web and flange element crippling stresses and areas:

$$f_{SCR} = \frac{\sum b_n t_n f_{ECR}}{\sum b_n t_n} \qquad (4)$$

2.3. Modifications for welding induced material properties

A key objective of analysing welded panel strength is to incorporate an allowance for the loss of material strength in the HAZ. A number of methods may be used to represent the potential loss of strength **[3]**. Due to its simplicity and ability to be incorporated within the standard conventional analysis, the so-called "equivalent section method" is used for the laser beam and friction stir welded panels.

The equivalent section method first assumes that the welded structure consists only of areas of HAZ material and areas of parent material. The HAZ material properties are assumed uniform with varying properties averaged across the zone. A factor k_z is introduced to relate the strength of parent and HAZ material, k_z being equal to the ratio of HAZ material proof stress to parent material proof stress. The k_z factor for a given HAZ is used in one of two ways:

a) Fully factored equivalent sections – The structure is analysed by factoring the thickness of the material in the HAZ by the appropriate value of k_z, and then applying parent properties to the resultant "equivalent" section. This approach is illustrated in Figure 3a. The analysis is simplified since only parent material properties are used in the calculations.

b) Parallel factored equivalent sections – The second approach is similar to that used in the classical bending theory of beams of dissimilar materials **[18]**. Only the thicknesses measured parallel to the neutral axis about which flexing will occur are factored while those measured perpendicular to the neutral axis remain unchanged, Figure 3b. In turn, but only when calculating the effective width of sheet working with the stiffener in the post-buckling domain,

the width of the HAZ in the sheet is factored while the thickness remains unchanged. Again only parent material properties are used in the calculations. This approach is more relevant to members with higher slenderness ratios, where member flexing is potentially significant.

Both equivalent section methods require parent material properties, the parent-HAZ material factor (k_z) and HAZ width (Z_N) data. It is important to note that the HAZ material factor (k_z) and HAZ widths (Z_N) are both material and welding process dependant and are a key input into any analysis. Without appropriate factors and widths, accurate and therefore 'safe' analysis is not assured.

2.4. Modifications for welding joint geometry

Using laser beam welding the resultant fabricated panel, Figure 2a, has no stiffener flange at the sheet-stiffener interface. The section crippling stress is calculated considering the free stiffener flange, stiffener web and sheet pad-up on to which the stiffener is welded as potential crippling elements. The sheet pad-up is only assumed a crippling element if the ratio of pad-up thickness to nominal sheet thickness is greater than 2, this is based on typical idealisation philosophy for integrally stiffened panels **[14]**.

For a friction stir welded panel however, the fabrication process requires a sheet-stiffener attached flange, Figure 2b. Therefore the crippling analysis must represent this attached flange and its connection with the panel sheet. In order to account for the welded sheet-stiffener joint two different joint idealisations are considered:

Joint Idealisation A (Figure 4a)

This is equivalent to the analysis of a riveted configuration where the stiffener is fastened to the sheet by two rows of rivets in a single flange. In this case the rivet lines are so close together that the effective width for each rivet line overlaps considerably. The crippling stress of the stiffener flange which is attached to the sheet is considered to have a thickness equal to 3/4 the sum of the

combined flange and sheet thickness **[14]**, as the sheet increases the stability of the attached flange. The stiffener crippling elements' assumed boundary conditions are then:

- Element 1 is assumed to have one edge simply supported and one edge free, buckling coefficient k = 0.64.
- Element 2 is assumed to have has both edges simply supported, k = 4.0.
- Element 3 is assumed to have one edge simply supported and one edge free, k = 0.64.

Joint Idealisation B (Figure 4b)

For joint idealisation B the stiffener is divided into four crippling elements. For Element 3 and 4 the element thickness is not changed to account for additional support offered by the sheet. The stiffener crippling elements' assumed boundary conditions are then:

- Element 1 is assumed to have one edge simply supported and one edge free, k =0.64.
- Element 2 is assumed to have both edges simply supported, k =4.0.
- Element 3 is assumed to have both edges simply supported, k =4.0.
- Element 4 is assumed to have one edge simply supported and one edge free, k =0.64.

The results of the modified analysis along with the experimental results are presented in the penultimate article section. The following section introduces the computational analysis methods.

3. Computational analysis methods

Using the FE method and employing non-linear material and geometric analysis procedures, it is possible to model the post buckling behaviour of stiffened panels without having to place the same emphases on empirical analysis methods **[19, 20]**. Therefore a competing computational method

will be assessed against the modified conventional analysis methods outlined in the previous section.

3.1. Idealisation

The idealisation approach adopted represents the stiffener web and flanges and the panel sheet as an assemblage of shell elements. This approach is essential to enable the crippling failure modes of the structure to be simulated **[19]**. Again the friction stir welded joints require special consideration of the sheet-stiffener joint idealisation. A number of idealisations for the sheet-stiffener weld joint are examined, Figure 5. In Idealisation 1 the weld joint is explicitly modelled, with nodes in the sheet and stiffener weld area connected with rigid links. This idealisation does not model the contact condition between the unwelded sheet and stiffener flange and therefore within the post-buckling domain the sheet and flange shells may penetrate each other. Idealisation 2 therefore models the weld plus the sheet and flange interface contact conditions. This is accomplished in ABAQUS with the remaining nodes at the interface linked using uni-axial gap elements, GAPUNI **[21]**.

3.2. Element Selection

To enable element selection a series of mesh convergence studies were undertaken. The buckling behaviour of uniformly compressed rectangular plates with geometries and boundary conditions designed to replicate those of the structure under investigation was analysed. Each analysis set was developed such that a theoretical buckling calculation could be preformed **[22]**. The performance of five ABAQUS elements were assessed based on convergence with corresponding theoretical behaviour with increasing mesh densities. Based on these analyses the first-order curved quadrilateral 4-noded finite strain general-purpose shell element, S4R **[21]** were selected.

3.3. Material Modelling

Within the previous conventional analysis method to account for the loss of material strength in the HAZ, equivalent sections were evaluated by factoring the geometry and assuming appropriate

parent material properties. In the FE analysis a material representation of reduced material properties within the HAZ is used, with the section geometry unchanged. The HAZ stress-strain curve is related to the parent curve through the factor k_z, which were obtained experimentally from previous work. Knowing the parent 0.1% and 0.2% proof stresses allows the HAZ material 0.1% and 0.2% proof stresses to be determined by factoring with k_z. Assuming the elastic modulus, E, to be constant, the remaining HAZ material properties (m and f_n) can then be determined. For a suitable range of strain values, parent and HAZ curves can be plotted using the Ramberg-Osgood equations. The full material stress-strain curves are then incorporated into the finite element analysis models using the 'classical metal plasticity' constitutive theory available within the ABAQUS material library.

3.4. Solution Procedure

For each analysis an initial eigenvalue analysis is performed to determine the fundamental buckling modes of the structure. The initial geometry is subsequently seeded with an imperfection in the shape of the fundamental buckling modes. Unless otherwise stated, the magnitude of this imperfection is 1% of the sheet thickness. The non-linear post buckling analysis is then performed using the incremental-iterative Newton-Raphson solution procedure **[23]**.

Reference 19 and 20 outline the development and stiffened panel sub-component experimental validation of the applied computational analysis procedures.

4. Experimental validation

In order to assess the accuracy of the proposed analysis methods an experimental validation programme was undertaken on laser beam and friction stir welded crippling specimens. Two specimen configurations were designed, manufactured and tested, one for each welding process. Due to the characteristics of the two welding processes, the specimens have different material combinations but similar geometric properties. The sheet thickness and stiffener dimensions are

representative of panel structure and the longitudinal stiffeners found on the lower fuselage belly of a mid-sized civil transport aircraft.

4.1. Specimen design

The laser beam welded specimen consisted of angle stiffener (6013-T6511 extrusion) welded to a flat sheet base (6013-T6) incorporating a pad-up (an area of sheet at the base of the stiffener with an increase thickness). The stiffener was attached to the sheet using a single sided full penetration weld, Figure 6. Partial recovery of material properties was obtained by welding in the naturally aged condition (T4), followed by an artificial ageing heat treatment process of the assembled welded specimens.

The friction stir welded specimens consist of a Z-section stiffener (7075-T76511 extrusion) welded to a flat sheet base (2024-T3) again incorporating a pad-up at the stiffener base. The stiffener was attached to the sheet using a lap weld with a partial penetration of the sheet, Figure 6. No post welding heat treatment process was carried out on the friction stir welded specimens, and a minimum period of time elapsed between specimen welding and specimen testing to ensure a stable state of natural ageing.

The welded specimens were designed to have slenderness ratios of approximately 10, thereby inducing specimen crippling failure. Table 1 gives the specimens' geometric properties and Table 2 gives the specimens' material properties. The compressive parent material properties were obtained from coupon tests, with the coupons taken from the same material batches as the specimen's sub-components.

4.2. Experimental procedures

The specimens were tested in a 250 kN capacity hydraulic, displacement-controlled compression-testing machine. A 25.4 mm thick Cerrobend (low melting point alloy) base was cast on to the 215.4 mm long welded specimens, producing fully clamped boundary conditions at each end.

Keying holes were drilled through the ends of the specimens prior to casting to hold the Cerrobend in position and to help prevent separation of the Cerrobend from the specimen. The ends were subsequently machined flat and perpendicular to the sheet to ensure that uniform axial loads were applied. No edge support members were used on the unloaded specimen edges given the potential for welding induced distortion and potential uncertainty in applied boundary conditions.

Two calibrated displacement transducers, one either side of the specimen, were used to measure specimen end-shortening. A number of specimens were strain gauged to determine local buckling behaviour. The specimens were loaded monotonically at a rate of approximately 10 kN/min until failure occurred, end-shortening and strain data being recorded automatically at 4-second intervals.

4.3. Modified conventional analysis

For the purposes of analysis the specimen sheet segments are assumed to be fully clamped along the loading edges at the edge of the cerrobend cast supports and free at the specimen edge, the sheet was conservatively assumed to be simply supported along the edge of the stiffener. For the laser beam welded specimen design, two analyses were performed, using the two equivalent section methods. Also, for the friction stir welded specimen design two analyses were performed, this time using the fully factored equivalent section method and the two joint idealisations outlined in Section 2. In addition, a complete set of analysis calculations were performed with $k_z = 1.00$, that is to say no reduced material properties within the HAZ, enabling a baseline from which to assess each method / idealisation.

4.4. Finite Element analysis

The loads and boundary conditions applied to the Finite Element models were designed to be as representative of the experimental test setup as possible, with the same loading and boundary conditions applied to each model. A uniform axial displacement was applied to one end of the model with the axial displacement at the opposite end restrained. Out-of-plane displacements of the nodes within the areas that were cast in Cerrobend in the experimental test were also restrained.

Compressive parent material properties obtained from coupon tests were used in all Finite Element analysis. For the friction stir welded specimen design two analyses were performed, one applying each joint idealisation outlined in Section 3. Again, as with the modified conventional methods, a complete set of analysis simulations were performed with 'no welding effects' as a baseline from which to assess each idealisation.

5. Results and Discussion

This section presents the analytical, numerical and experimental results for the laser beam and friction stir welded panels respectively.

5.1. Laser beam welded specimens

Table 3 presents the experimental specimen crippling failure loads along with the predicted conventional and finite element crippling loads. Figure 7 presents the load versus end shortening curves for the experimental specimens and the finite element analysis. Considering first the experimental behaviour, all three specimens failed in crippling, Figure 9, and at similar load levels, Table 3. Significantly, for all specimen tests the sheet-stiffener weld remained intact into the specimen post failure region.

Examining the modified conventional crippling analysis methods, the fully factored equivalent sections method under predicts the failure strength of the structure, with the parallel factored equivalent sections method slightly over predicting. Analysis with no welding material effects (k_z = 1.00) results in a larger over prediction. Typically for riveted structures the conventional analysis results in a conservative estimate of ultimate load. Given the over prediction, clearly the standard stiffened panel buckling analysis procedures must at minimum be altered to account for the welding modified material properties. To fully qualify a design an additional safety factor or experimental validation programme should be considered.

Considering the finite element results, the model predicts a pre-buckling stiffness which is equivalent to a near perfect structure (magnitude of seeded imperfection only 1% skin thickness) with no welding induced residual stresses or resultant distortions. The experimental stiffness curves for all three specimens under perform in comparison with this perfect structure as would be expected. Examining the post-buckling stiffness, the model again predicts for a perfect structure and again appears overly stiff in comparison to the experimental behaviour. By not representing the welding induced residual stresses and resultant distortions within the model, the analysis fails to predict the welded specimen's true stiffness. Ultimately the finite element model over predicts the specimen failure, but predicts a similar failure mode shape, Figure 9.

5.2. Friction stir welded specimens

Figure 8 presents the load versus end shortening curves for the experimental specimens and the finite element analysis. All three experimental specimens failed in crippling, Figure 9, and at similar load levels, Table 4. Again as with the laser beam specimens all sheet-stiffener welds remained intact into the specimen post failure region.

Examining the modified conventional analysis methods, both for Idealisation A and B, the fully factored equivalent sections method over predicts the failure strength of the structure. Considering the finite element results, both Idealisations 1 and 2 predict pre-buckling stiffness equivalent to a perfect structure with no welding induced residual stresses or resultant distortions. The experimental stiffness curves for all three specimens under perform in comparison with this near perfect structure. Examining the post-buckling stiffness, the models initial predictions are overly stiff in comparison to the experimental behaviour. Towards the collapse load both models representing the HAZ properties under predict the specimen experimental stiffness. Idealisation 1 which does not represent the contact conditions at the stiffener-sheet interface fails at a much lower load and end-shortening than found experimentally. Idealisation 2 which represents the contact

conditions predicts a larger failure load but less than the lowest specimen (FS3). The variation in finite element results indicates that the contact conditions at the sheet-stiffener should be modelled.

It is worth noting that the laser beam welded specimen's strength was over predicted by the FE analysis, whereas the friction stir welding specimen's strength was under predicted. This may relate to the larger HAZ width associated with the friction stir welded specimens and the general assumption and idealisation that the HAZ has a uniform material property distribution, with properties averaged across the zone. This may be more appropriate for the analysis of the laser beam welded panel, with its relatively small HAZ width. Again, as highlighted before, not representing the welding induced residual stresses and resultant distortions limits the accuracy of the finite element predictions.

6. Conclusions

The aim of this study was to develop and assess analysis methods, accounting for the loss of material strength in the HAZ, for the crippling failure of stiffened panels fabricated using laser beam and friction stir welding. Two analysis methods have been formulated, one based on modifications to conventional empirical methods, and one based on the finite element method. Both approaches have been examined against experimental data. The experimental work has demonstrated the static strength of the laser beam and friction stir welded sheet-stiffener joints under buckling collapse loads. For each specimen tested, weld joint integrity was maintained throughout local skin buckling, post buckling, and ultimately overall specimen crippling.

Considering analysis with modified empirical methods, the standard stiffened panel buckling analysis procedures must be altered to account for the weld joint geometry and material properties. For the examined specimens, the predictions of strength were reasonably close to the experimental results, with scatter of +2.1% to –1.6% the lowest experimental values. It is important to note that the basic conventional analysis methods, into which the modifications are incorporated, are

empirical in nature. Ultimately the inherent weaknesses and uncertainties with the conventional analysis methods in terms of empirical data and simplifying assumptions remain. In addition, the modified methods do not account for any welding induced residual stresses or resultant distortions. Finally, the modified methods assume uniform material property distributions in the HAZ with properties averaged across the zone, this may be appropriate for the analysis of welded panels with relatively small HAZ widths, but may introduce increased uncertainties for panels with larger HAZ widths.

Considering the proposed computational methods, non-linear finite element analysis procedures may be used to accurately model the crippling collapse behaviour. As with the modified empirical methods, welding altered material properties and weld joint geometry must be accurately represented. Additionally for friction stir welded panels, the contact conditions at sheet-stiffener joint interfaces must be represented. The methods developed and validated do not consider welding induced residual stresses or resultant distortions and it has been demonstrated that these are necessary for accurate consistent results. Further work is required to modify the finite element analysis procedures to consider geometric distortion and residual stress properties due to both the laser beam and friction stir welding process **[24]**.

Acknowledgements

The authors gratefully acknowledge the support of Bombardier Aerospace Belfast and in particular Gary Moore and Ken Poston from the Materials and Processes Engineering Department.

References

1 **Irving, P.** End of the aircraft rivet-the coming of the welded aircraft, *Aerogram*, Vol. 10, No. 2, pp. 10-13, September 2001.

2 **Mendez, P.F., and Eagar, T.W.** Welding Processes for Aeronautics, *Advanced Materials & Processes*, pp 39-43, May 2001.

3 **Gibson, A.** An investigation into the compressive strength and stability characteristics of welded aircraft fuselage panels. *PhD Thesis*, Queen's University Belfast, N. Ireland, 2000.

4 **Zink, W.** Laser beam welding for aircraft structures. *Aeromat 2000*, Daimler Chrysler Aerospace Airbus, Bremen, 2000.

5 **Midling, O.T.** Material flow behaviour and microstructural integrity of friction stir butt weldments. Proceedings of the 4th International Conference on *Aluminium Alloys*, Atlanta, pp. 451–458, 1994.

6 **Peel, M., Steuwer, A., Preuss, M. and Withers, P.J.** Microstructure, mechanical properties and residual stresses as a function of welding speed in aluminium AA5083 friction stir welds, *Acta Materialia*, Vol. 51, pp 4791–4801, 2003.

7 **Eurocode 9**, Design of aluminium structures, part 1-1: General rules, 1998.

8 **British Standard**, BS8118: Structural Use of Aluminium: Part 1, 1991.

9 **Gourd, L.M.** *Principles of Welding Technology*, Third Edition, Arnold, London, 1995.

10 **Zink, W.** Welding fuselage shells, *Industrial Laser Solutions*, April 2001.

11 **Dracup, B.J. and Arbegast, W.J.** Friction Stir Welding as a Rivet Replacement Technology, Proceedings of the *1999 SAE Aerospace Automated Fastening Conference & Exposition*, Memphis, TN, October 5-7, 1999.

12 **Hoffman, E.K., Hafley, R.A., Wagner, J.A., Jegley, D.C., Pecquet, R.W., Blum, C.M. and Arbegast, W.J.** Compression Buckling Behaviour of Large-Scale Friction Stir Welded and Riveted 2090-T83 Al-Li Alloy Skin-Stiffener Panels, NASA/TM-2002-211770, *NASA Washington*, DC, August 2002.

13 **Rhodes, J. and Walker, A.C.** *Developments in thin-walled structures*, Chapter 4 - Effective widths in plate buckling pp 119-157, Applied science publisher, London, 1982.

14 **Bruhn, E.F.** *Analysis and design of flight vehicle structures*. 1st edition, Tri-State Offset Company, 1973.

15 **NASA**, NASA Astronautics structures manual, Volume 3, NASA, Washington, US, 1961.

16 **ESDU Structures sub-series**, Engineering Sciences Data Units, ESDU International Ltd.

17 **Ramberg, W. and Osgood, W.R.** Description of Stress-Strain Curves by Three Parameters, NACA-TN 902, *National Advisory Committee for Aeronautics (NACA)*, Washington, USA, 1943.

18 **Benham, P.P., Crawford, R.J. and Armstrong, C.G.** *Mechanics of engineering materials*, Longman Scientific and Technical, London, 1996.

19 **Lynch, C., Murphy, A., Price, M. and Gibson, A.** The computational post buckling analysis of fuselage stiffened panels loaded in compression, *Thin-Walled Structures*, Vol. 42:10, pp 1445-1464, 2004.

20 **Murphy, A., Price, M., Lynch, C., and Gibson, A.** The computational post buckling analysis of fuselage stiffened panels loaded in shear, *Thin-Walled Structures*, Vol. 43:9, pp 1455-1474, 2005.

21 Anonymous. *ABAQUS / Standard user's manual*. Version 6.1, Hibbitt, Karlsson and Sorenson, 2000.

22 **Bulson, P.S.** *The stability of flat plates*, 1st edition, Chatto & Windus, London, 1970.

23 **Becker, A.A.** *Understanding non-linear finite element analysis – Through illustrative benchmarks*, 1st edition, NAFEMS (ISBN 1-8743-7635-2), 2001.

24 **Murphy, A., Price, M., and Wang, P.** The Integration of Strength and Process Modeling of Friction-Stir-Welded Fuselage Panels, AIAA-2005-2026, *46th AIAA/ASME/ASCE/AHS/ASC Structures, Structural Dynamics, and Materials Conference*, Austin, Texas, April 2005.

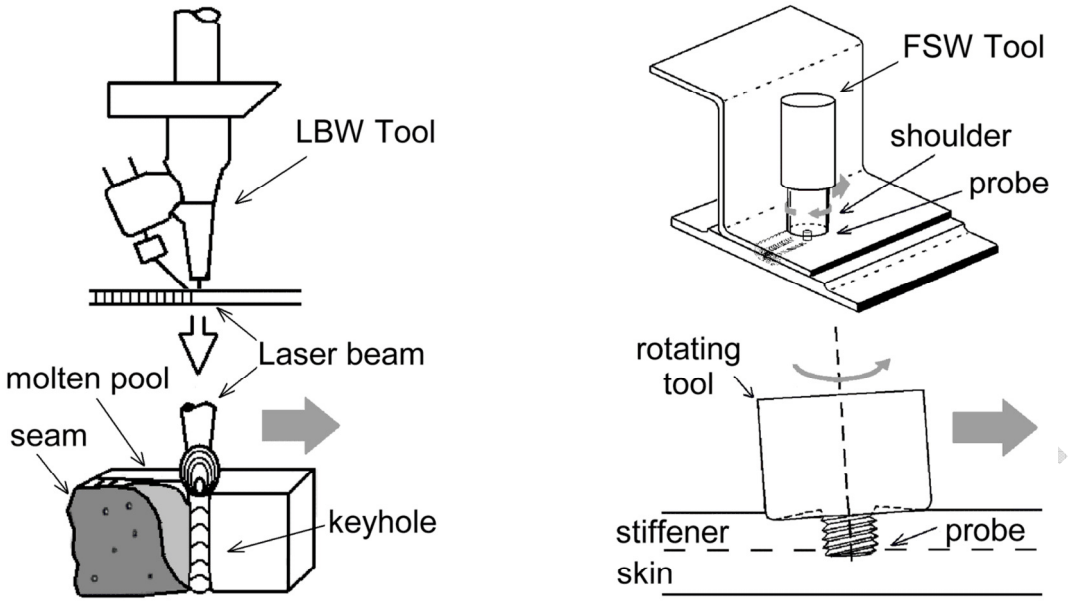

a) The laser beam welding process. *b) The friction stir welding process.*

Fig. 1. The welding processes.

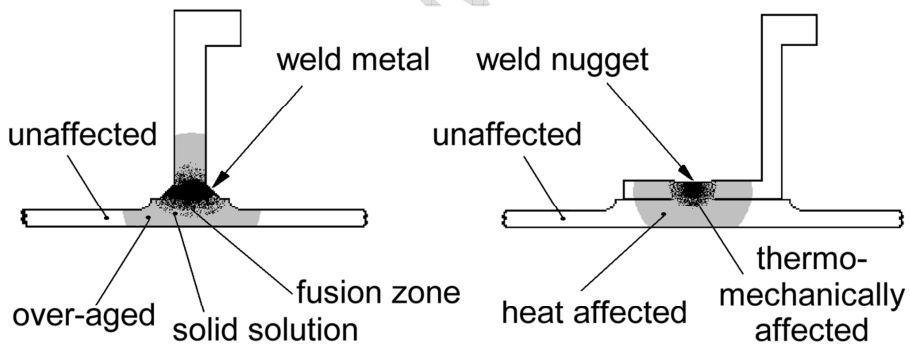

a) Laser beam welded section. *b) Friction stir welded section.*

Fig. 2. Schematic of weld transverse cross-section.

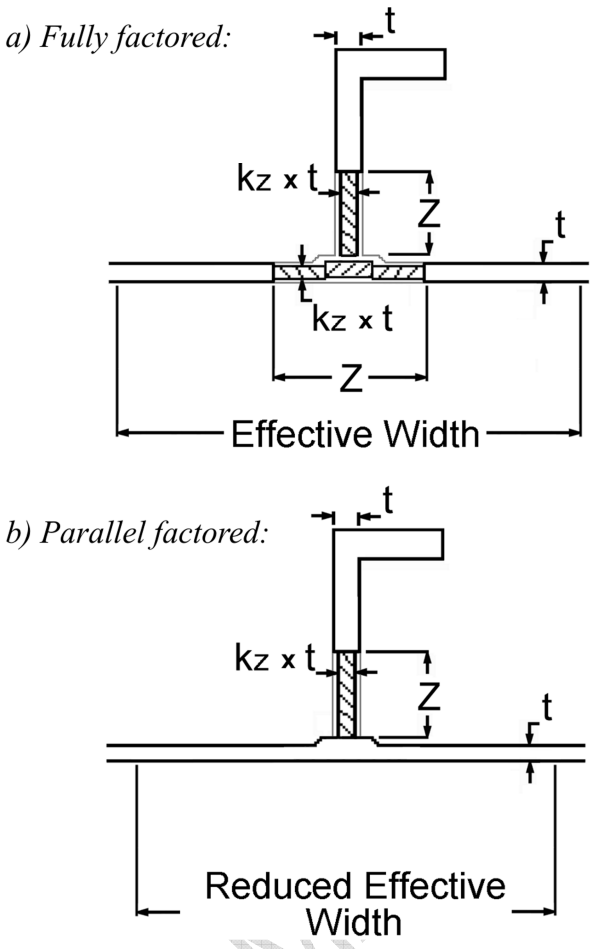

Fig. 3. Equivalent section methods.

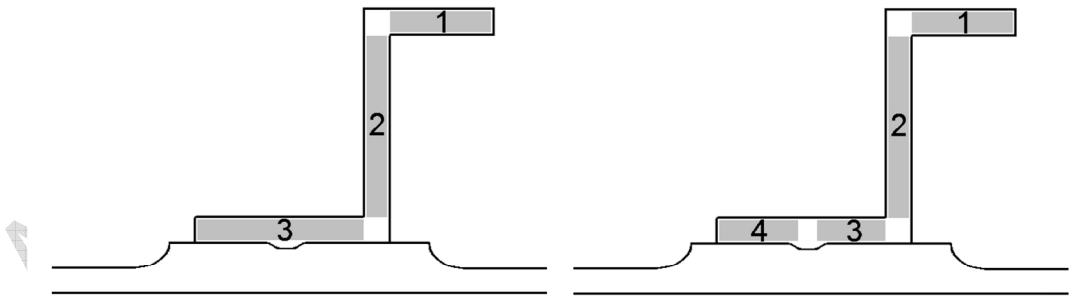

a) Idealisation A. *b) Idealisation B*

Fig. 4. Joint idealisation (Friction stir welding).

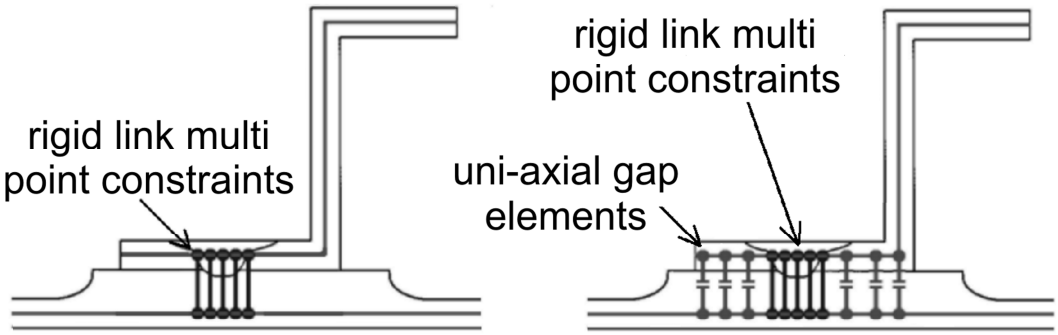

a) Idealisation 1. *b) Idealisation 2.*

Fig. 5. FE sheet-stiffener interface idealisation (Friction stir welding).

a) Laser beam welded specimen:

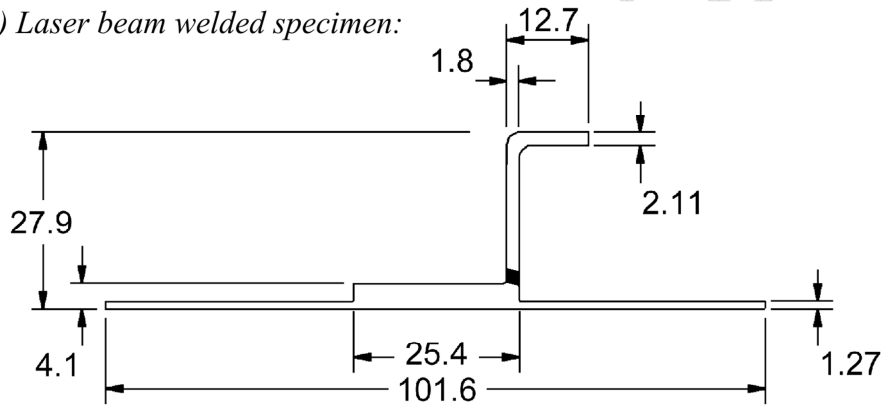

b) Friction stir welded specimen:

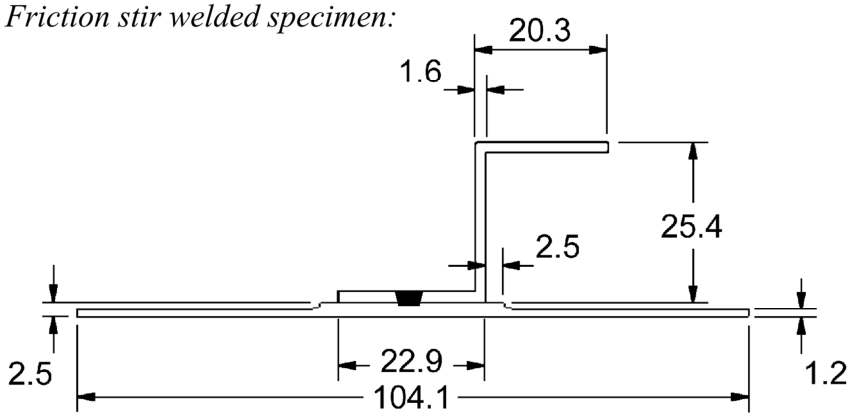

Fig. 6. Crippling specimen geometry (All dimensions in millimetres).

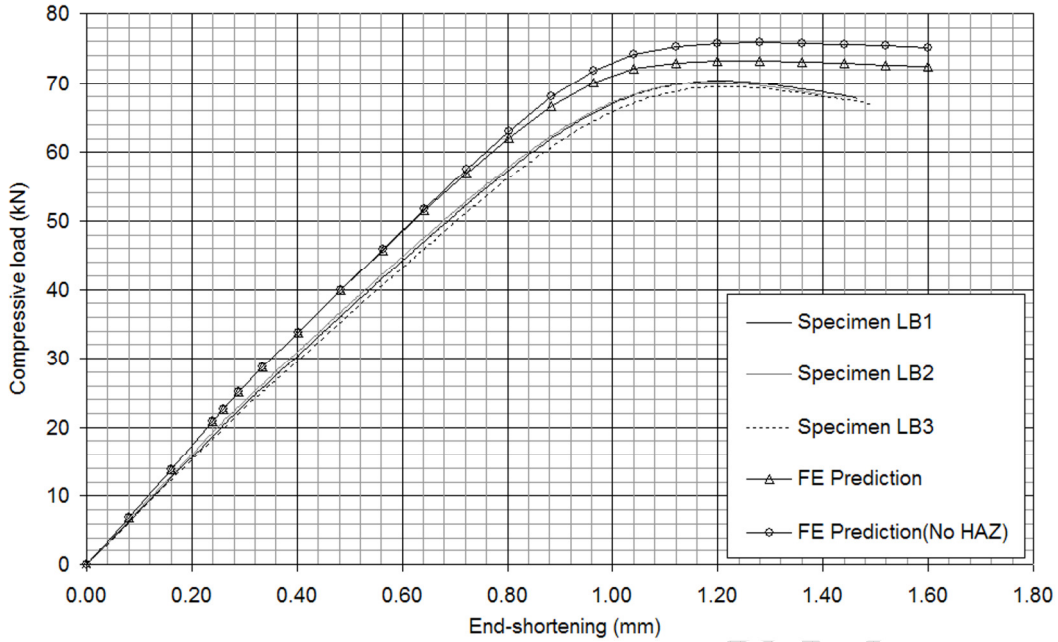

Fig. 7. Load versus end-shortening curves (Laser beam welded).

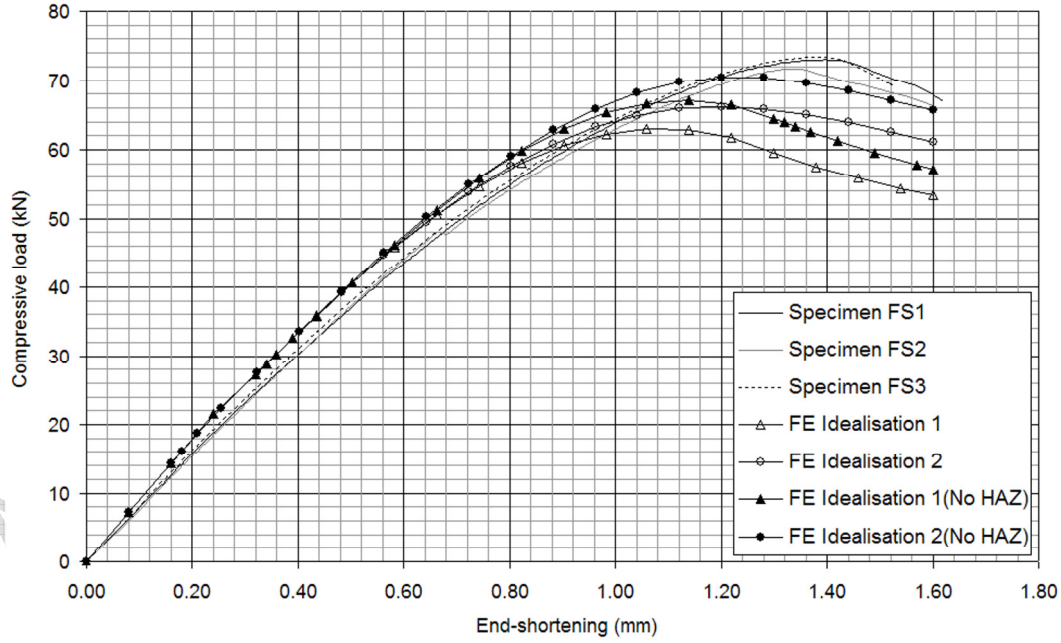

Fig. 8. Load versus end-shortening curves (Friction stir welded).

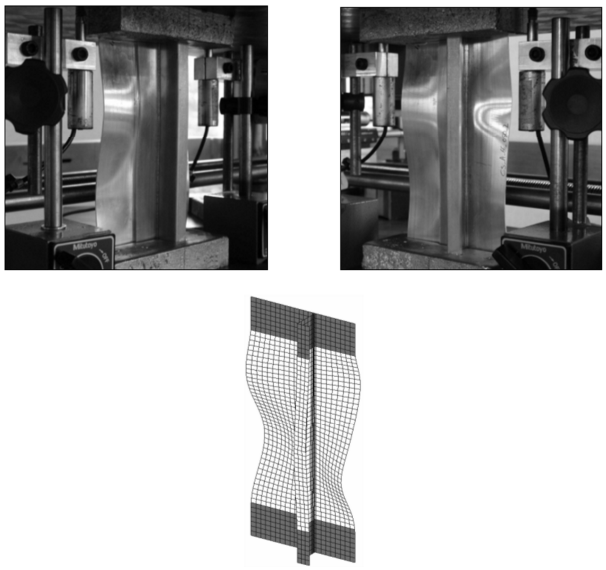

a) Laser beam welded (Specimen LB2)

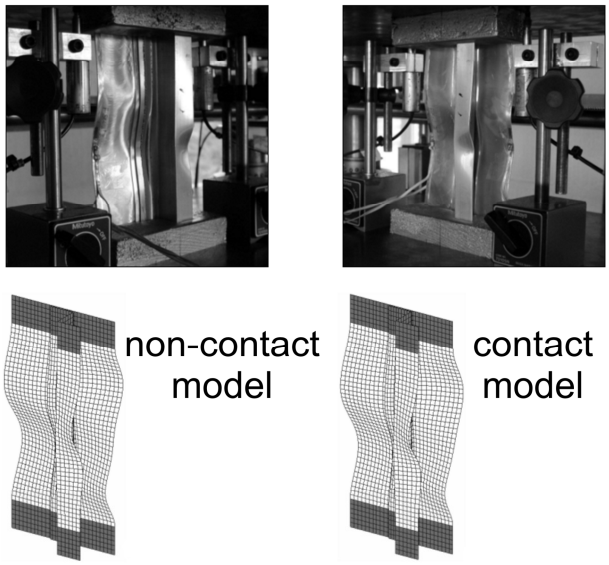

b) Friction stir welded (Specimen FS2)

Fig. 9. Specimen failure modes.

	Sheet thickness (mm)	Cross sectional area (mm^2)	Percentage difference (%)[1]	Slenderness ratio[2]	Percentage difference (%)[1]
Laser beam specimens	1.27	267		9.3	
			0.4		5.4
Friction stir specimens	1.2	266		8.8	

[1] *laser beam specimen taken as baseline*
[2] *calculations performed on un-factored cross-sectional geometry*

Table. 1. Crippling specimen geometric properties.

	Laser beam specimens		Friction stir specimens	
Material	6013-T6	6013-T6511	2024-T3	7075-T76511
Young's Modulus (**E**) (GPa)	72.4	69.0	68.6	71.4
Poisson's Ratio (**ν**)	0.33	0.33	0.33	0.33
Compression yield stress ($\mathbf{f_{CY}}$) (MPa)	359.2	360.9	335.4	482.6

Table. 2. Crippling specimen parent material properties.

	Load (kN)	Average stress (MPa)[1]	Percentage difference (%)[2]
Experimental			
Specimen LB1	70.3	263	+1.2
Specimen LB2	70.2	263	+1.0
Specimen LB3	69.5	260	---
Conventional			
No weld effects considered	72.8	273	+4.8
Fully factored equivalent sections	68.4	256	–1.6
Parallel factored equivalent sections	69.7	261	+0.3
Computational			
No weld effects modelled	75.9	284	+9.2
HAZ modelled	73.3	275	+5.5

[1] *- Based on the individual initial specimen cross-sectional areas – Table 1.*
[2] *- Based on lowest experimental failure load (specimen LB3)*

Table. 3. Crippling failure load (Laser beam welded).

	Load (kN)	Average Stress (MPa)[1]	Percentage difference (%)[2]
Experimental			
Specimen FS1	73.0	274	+1.8
Specimen FS2	71.7	270	---
Specimen FS3	73.4	276	+2.4
Conventional			
No weld effects considered			
Idealisation A	78.3	294	+9.2
Idealisation B	78.1	294	+8.9
Fully factored equivalent sections			
Idealisation A	73.2	275	+2.1
Idealisation B	73.1	275	+2.0
Computational			
Idealisation 1 (No weld effects)	67.1	252	–6.4
Idealisation 2 (No weld effects)	70.4	265	–1.8
Idealisation 1 (HAZ modelled)	63.0	237	–12.1
Idealisation 2 (HAZ modelled)	66.2	249	–7.7

[1] *- Based on the individual initial specimen cross-sectional areas – Table 1.*
[2] *- Based on lowest experimental failure load (specimen FS2)*

Table. 4. Crippling failure load (Friction stir welded).